RECOIL PROPERTIES OF Bi^{209}(p,pxn) SPALLATION PRODUCTS

William R. Pierson

and

Nathan Sugarman

THE UNIVERSITY OF CHICAGO

THE ENRICO FERMI INSTITUTE FOR NUCLEAR STUDIES

DISCLAIMER

EFINS-62-79

The Enrico Fermi Institute
for Nuclear Studies

THE UNIVERSITY OF CHICAGO
Chicago, Illinois

RECOIL PROPERTIES OF $Bi^{209}(p,pxn)$ SPALLATION PRODUCTS

William R. Pierson

and

Nathan Sugarman

Enrico Fermi Institute for Nuclear Studies and
Department of Chemistry, University of Chicago,
Chicago, Illinois

Facsimile Price $ 5.60
Microfilm Price $ 1.85

Available from the
Office of Technical Services
Department of Commerce
Washington 25, D. C.

Recoil Properties of Bi^{209}(p,pxn) Spallation Products*

William R. Pierson† and Nathan Sugarman
Enrico Fermi Institute for Nuclear Studies,
University of Chicago,
Chicago, Illinois.

ABSTRACT

Recoil properties of products of Bi^{209}(p,pxn) reactions at a bombarding proton energy of 450 Mev have been measured and compared with those predicted from the Monte Carlo cascade calculations of Metropolis et al. Agreement is good, although it appears that the calculation overestimates the transverse momentum component and does not predict as rapid a change in this component with mass number as that observed.

The effect on the results caused by scattering of the recoiling nuclei during the stopping process is shown to be important.

Approximate values for the yield ratios Bi^{205}/Bi^{206}, Po^{205}/Bi^{205}, and Po^{206}/Bi^{206} are presented. The latter two seem higher than those previously reported.

I. INTRODUCTION

Reactions of nuclei with particles of kinetic energy of the order of 100 Mev are thought to proceed by a two-step process first suggested by Serber[1]. In the first step, commonly called the cascade, or prompt cascade, the incident particle makes collisions with individual nucleons and generates a prompt shower or cascade of fast nucleons, some of which may escape the nucleus. The residual nucleus is left with excitation energy, usually much less than the bombarding energy, and some kinetic energy. The second step is the loss of excitation energy by particle evaporation and gamma-ray emission. Fission may occur during de-excitation. Monte Carlo calculations of the cascade step have been performed [2] for a variety of nuclei and bombarding energies in order to provide a basis for testing this description of high-energy nuclear reactions. These calculations can be made to yield estimates for the probabilities (cross sections) for formation of the various possible product nuclei and the momenta of these nuclei, provided that the effects of the de-excitation step are considered. Cross section measurements have been made [3-7] and many have been compared with the Monte Carlo calculations. However, the momentum predictions[8,9] of the Monte Carlo calculations[2] have been less extensively studied[8-12]. The purpose of the work reported in this paper is to obtain recoil data[13] for certain spallation products, as a test of the momentum

predictions of the Monte Carlo calculations. The products of Bi^{209}(p,pxn) reactions (where the notation (p,pxn) signifies also all other reactions which lead to the same products — (p,pπ°xn) or(p,$\pi^{\pm}$(x+1)n), for example) at a bombarding proton energy of 450 Mev were investigated. The results obtained are consistent with the results of earlier experiments[14] and in fair agreement with the Monte Carlo predictions[8,9].

II. EXPERIMENTAL METHOD

The irradiations, two hours in length, were done in the circulating beam of the 450 Mev proton synchrocyclotron of the University of Chicago. The recoil target assemblies irradiated may be distinguished as "thick-target" or "thin-target", depending on whether W, the thickness of the bismuth target, is large or very small compared to the ranges of the recoil nuclei.

Both types of assemblies employed catcher foils of sufficient thickness to stop all recoil nuclei which escape from the bismuth. The two types of assemblies are depicted in Figs. 1 and 2, where T indicates the bismuth targets, F and B (or U and D) the forward and backward (or up and down) catchers, respectively, A the activation foils, and G the guard foils. The whole assembly was wrapped in 1-mil aluminum. The thick bismuth targets (Fig. 1) were prepared by rolling 5.5-mil

bismuth ribbon, with frequent heating, down to about 1.2 to 1.8 mil (W ~ 30 to 45 mg/cm^2) and cutting out pieces from this with a template, usually 1.5 cm x 2.0 cm. The targets prepared in this way are not brittle and appear to have very smooth surfaces. The value of W was determined by weighing and dividing by the known area, and should be accurate to about 2%, exclusive of inhomogeneities.

The catcher foils were either of 6.9 mg/cm^2 (1 mil) aluminum or 2.6 mg/cm^2 (0.05 mil) gold, of dimensions adequate (2.0 cm x 2.5 cm) to overlap the edges of the bismuth targets in the assembly and thus catch all recoils escaping the bismuth. Activation foils identical to the catchers were included for correcting for impurities in the catchers which might give rise to the product activities being scrutinized. Guard foils of gold were used in those cases in which the catchers were gold; otherwise they were dispensed with, since the wrapper of the assembly was of the same material as the catchers. The possibility of effects arising from thin places or pinholes in the gold foils was checked by carrying out an experiment with a stack of these foils as catchers. The results showed no evidence of these effects.

The thin bismuth targets were prepared by evaporating a thin film (about 0.2 μg/cm^2) of bismuth, 2.5 cm x 2.5 cm, onto 3.2 cm x 3.2 cm aluminum or gold foils. These latter foils served as catcher foils, as shown in Fig. 2. Since

targets sufficiently thin to allow escape of more than about 95% of the recoils could not be achieved, it was necessary to have two complete sub-assemblies in each thin-target assembly, with the target evaporated onto the backward catcher in one sub-assembly and onto the forward catcher in the other, as shown. The evaporations were carried out for both targets simultaneously and in such a way that the thicknesses deposited were always within 10% of each other as estimated from the total activity produced. With this arrangement, it was a simple matter to correct for the effect of thickness of the target, by subtracting the calculated target activity from the activity of the foil on which the target had been deposited.

The bismuth used in the thick-target experiments was cleaned before rolling and again afterwards by washing in 0.5M HNO_3, water, and acetone. After the target assembly had been put together, it was stored in vacuum until bombardment time. Failure to observe these precautions and to clean the rollers carefully ordinarily led to large errors. For example, allowing a target assembly to stand in the open air for about 6 months prior to bombardment resulted in a reduction of about 15% in the amount of activity escaping from the target.

There is some evidence from this laboratory[15] that increases in catcher-foil activity may be observed in thick-target experiments on magnesium, phosphorus, and potassium recoils from a copper target if the target foil has a rough

surface of coarseness comparable to the recoil ranges being measured. Measurements for Bi^{203} using rough and smooth bismuth targets did not show this effect. Of greater importance were high values of catcher-foil activity in thick-target experiments when the target was so thick (~5 mil) that the number of recoil nuclei escaping from the edges of the target foil was appreciable. Most of these recoils are stopped in the catcher foils; for 5.5-mil bismuth targets this results in catcher-foil activity values some 5 to 10% higher than the correct values in the case of the backward catcher foil, and 1 to 2% in the case of the forward catcher foil. This effect is not serious for the target thicknesses (~1.5 mil) used in these experiments.

The thick-target assemblies were oriented as shown in Fig. 1(a) for the "forward-backward" experiments, and as shown in Fig. 1(b) for the "perpendicular" experiments. For the latter experiments, the plane of the assembly is canted at 10° to the incoming beam rather than parallel to it, in order to avoid a decrease of the beam intensity deep inside the target from multiple scattering. If this precaution is not taken, the measured catcher-foil activities will be higher than they should be.

The maximum intensity of the circulating beam for thick-target runs was about 1/8 full beam, so chosen to avoid

melting the bismuth. Lower beam intensities gave the same recoil results, indicating that thermal effects are unimportant at 1/8 full beam. On the other hand, it was apparent from comparison of thin-target runs at various intensities that the recoil results in that case were independent of beam intensity; consequently the thin-target assemblies were irradiated at full beam.

After irradiation, the assembly was taken apart, the foils were dissolved and a known weight of bismuth carrier was added to each solution. Separation of bismuth (see Appendix) was begun immediately in order to minimize the contribution of polonium precursors. Later steps in the separation were delayed until the bismuth isotopes of mass A < 203 had mostly decayed away. The final precipitates were weighed in order to determine the radiochemical yield. These precipitates then were dissolved and known weights of lead carrier were added. The lead daughters 52-hr Pb^{203} and 68-min Pb^{204m} were then removed from their bismuth parents (both about 12-hr) after an appropriate period (about 33 hours for Pb^{203}, four hours for Pb^{204m}) and purified (see Appendix), and the yields determined gravimetrically. The bismuth parent fraction was then precipitated about 5-6 days later for the determination of Bi^{205} and Bi^{206}. The samples, normally about 10 mg/cm^2 thick, were mounted on aluminum cards and counted with gamma-ray spectrometers.

Decay of Pb^{203} generally was followed for about seven half-periods. Decay-curve analysis was necessary for Pb^{204m}, Bi^{205}, and Bi^{206}. The latter two species were counted for about four months, beyond which time background problems made it impracticable to continue. Duplicate analyses were usually done on all but the backward-catcher and activation foils, and agreement was usually better than 1% for the bismuth samples and 4% for the lead samples.

The determination of the recoil properties of Bi^{203} (via Pb^{203}), Bi^{205}, and Bi^{206}, was made with 1/8" thk x 1-1/2" diameter NaI(Tl) crystals as detectors. The single-channel spectrometers were set to accept the K x rays accompanying the electron-capture decay of these species. For Bi^{204} (via Pb^{204m}), a 7/8" thk x 1-1/2" diam NaI(Tl) crystal was used and the spectrometer was set for the peak of the 375-kev gamma ray which follows the isomeric transition. The energy selection and the use of crystals of minimal thickness, together with shielding, reduced the background to 3.3 to 8 counts per minute, depending on the crystal and channel setting. The phototubes used (EMI 9536B) have no measurable gain dependence on counting rate, at least over the range of rates encountered in this investigation. The instruments were checked frequently with appropriate standards, and minor electronics adjustments were made as needed to keep the window of the single-channel analyzer centered at the proper energy and of the proper width.

Simultaneous counting of the gross activity was performed with another scaler, the purpose of which was the determination of the coincidence correction ($\tau \sim 6$ μsec) and the parallel collection of data.

The results of these experiments are reported in the following terms: If F_X equals the activity of a given species in catcher-foil X divided by the total activity of that species in the entire assembly, then for the thick-target experiments (see Fig. 1) the quantities $F_F W$, $F_B W$, $F_U W$, and $F_D W$ (and the average $F_P W$ of $F_U W$ and $F_D W$) are given. For the thin-target experiments (Fig. 2) the quantity F_F is given ($F_B = 1 - F_F$ for $W = 0$).

III. RESULTS

A. Preliminary Experiments

Preliminary experiments were conducted for the purpose of ascertaining the extent that thermal effects (during bombardment) and polonium precursors affect the results.

1. Thermal effects. As mentioned earlier, bombardments conducted with high- and low-intensity beams were found to give the same recoil results, indicating that thermal effects were of no consequence in this work. The following experiment was performed to make this point more secure.

A foil of bismuth was irradiated with 450-Mev protons for two hours and then clamped between several sheets of 2.6 mg/cm^2 Au. This stack of foils was allowed to stand for a few hours at room temperature, 100°C, and 200°C, counting the gold foils after each period. Noticeable activity was found in the gold foils after heating at 100°C, and considerably more after heating to 200°C, with substantial amounts appearing in the farther foils. Gamma-ray spectra of the foils indicated that the chief component was probably the K x-ray of an element in the neighborhood of bismuth; subsequent chemical separations showed that the activity was not bismuth. Therefore thermal effects play no role in the case of bismuth, but this may not be true for recoil nuclei of nearby elements.

2. Polonium precursors. Polonium was removed as soon as practicable (about one hour) after bombardment (see Appendix). Nonetheless, a sizable part of the observed bismuth activity is formed from decay of polonium, judging from cross section data[3,4,7]. Therefore, it was deemed advisable to test the effect of polonium precursors on the bismuth recoil results. This was done by isolating a set of Bi^{205} and Bi^{206} samples at the usual time, and comparing the F_FW values with the F_FW values obtained from a set in which the chemical separation of bismuth from polonium was delayed several days.

The contribution of polonium precursors caused the activity in the second set of samples to be some 13 to 14%

(depending on the time) higher than that in the first set. The F_FW for Bi^{205} was 0.7% lower, which is not significant. However the F_FW for Bi^{206} was 6% lower, which implies that the F_FW for Po^{206} must be about half that for Bi^{206}. The accuracy ($\pm 2\%$) of the measurements limits the F_FW disparity between Po^{205} and Bi^{205} to $\leq 25\%$.

From these results it follows that polonium has a negligible effect on the F_FW of Bi^{206} determined in the usual way (i.e. with samples separated soon after bombardment), because only about 0.16% of the Bi^{206} in that case is formed by Po^{206} decay. The error in F_FW for Bi^{205} as normally measured is less than 4%, estimated from the measured Po^{205}/Bi^{205} yield ratio and the aforementioned limit of disparity in F_FW between Po^{205} and Bi^{205}. (About 18% of the Bi^{205}, when separated at the usual time, is formed from Po^{205} decay.)

If the isobaric yield ratio and difference in recoil behavior between polonium and bismuth at mass number 205 are typical of mass numbers 204 and 203, then the maximum errors in F_FW attributable to polonium precursors should be about 3% and 7% for Bi^{204} and Bi^{203} respectively. However, the data for mass numbers 205 and 206 suggest that the disparity in F_FW between polonium and bismuth might decrease with mass number, in which case the errors for Bi^{204} and Bi^{203} would be less than these figures.

Half-periods adopted for these calculations are: 15 day for Bi^{205} and 6.0 day for Bi^{206}, as determined in the present work; 1.8 hr for Po^{205} and 8.8 day for Po^{206}, from the Nuclear Data Sheets[16].

The yield ratios Po^{205}/Bi^{205}, Po^{206}/Bi^{206}, and Bi^{205}/Bi^{206} were calculated from these experiments and are presented in Table I. For the Bi^{205}/Bi^{206} yield ratio, it was necessary to make an assumption regarding the counting efficiencies. Equal counting efficiencies (within $\pm 20\%$) were assumed for the two species with the counting arrangement used (counting K x rays with the source 0.1 cm from a 1/8"-thick crystal). The Bi^{205}/Bi^{206} ratio is concordant with earlier work[4]. The Po^{205}/Bi^{205} and Po^{206}/Bi^{206} yield ratios are, however, higher than those calculated from published[3,4] data. Recent measurements[7] at a proton energy of 135 Mev give Po^{205} and Po^{206} yields which are much higher (about 70 mb) than those found by Hunter and Miller[4] (about 10 mb) at 380 Mev.

B. Recoil Measurements

The experimental data are presented in Tables II and III. Three determinations of thick-target $F_F W$ values for composite samples of Bi^{205} and Bi^{206} with aluminum catcher foils gave results identical with values obtained from three similar experiments with gold catcher foils. Therefore, Table II shows the thick-target data averaged without regard to the catcher-foil material. However, the results of the thin-target

experiments depend strongly on the catcher-foil material, as is apparent in Table III. Therefore, Table II shows the thin-target data for aluminum catchers only. The errors quoted in the tables are the estimated standard deviations of the mean due to random errors. They do not include systematic errors due to polonium precursors or, for thick-target experiments, target surface effects. The number of acceptable determinations made for the F_FW and F_BW values given in Table II are: mass 203,3; mass 204, 3; masses 205 and 206, 6; for the F_PW values of Table II: mass 203, 4; masses 205 and 206, 1; and for the F_F values: masses 203, 205, 206, 1 each.

For the data of Table III, an initially pure bismuth fraction was isolated at the same time after the end of bombardment in each case (6 hr) and counted about 2 hours later. In this way the several decay chains present (mostly mass numbers 203 and 204, with some 201 and 202) were always present in the same proportions for each run at the time of counting, enabling the effect of the catcher-foil material to be studied without having to isolate any particular nuclide. The number of acceptable determinations made for the quantities given in Table III are: Al_B-Al_F, 6; Al_B-Au_F, 2; Au_B-Au_F, 1; Au_B-Al_F, 1.

TABLE I.

Ratios of yields of bismuth and polonium isotopes of masses 205 and 206.

	Ratio[a]	No. of determinations	Ratios from literature data	
			Bennett[b]	Hunter & Miller[c]
Bi^{205}/Bi^{206}	0.93 ± 0.20[d]	1		1.014 ± 0.186
Po^{205}/Bi^{205}	0.39 ± 0.06	2	0.133	0.258 ± 0.192
Po^{206}/Bi^{206}	0.28 ± 0.15	2	0.125	0.156 ± 0.115

a. Most of the quoted error arises from uncertainties in the half-periods or, for Bi^{205}/Bi^{206}, relative counting efficiencies.

b. Reference 3. This work was done with 375- and 450-Mev protons.

c. Reference 4. This work was done with 380-Mev protons.

d. Counting efficiencies for Bi^{205} and Bi^{206} were assumed to be equal, within $\pm$ 20% (see text).

TABLE II.

Recoil Results.

Nuclide	Species counted	Thick target, Al and Au catchers					Thin target, Al catchers	
		$F_F W$	$F_B W$	$F_U W$	$F_D W$	$F_P W$[a]	F_F	F_F/F_B
Bi^{203}	52-hr Pb^{203}	0.0434	0.0057	0.0261	0.0217	0.0239	0.8275	4.80
		±0.0004[b]	±0.0002	±0.0009	±0.0007	±0.0006	±0.0027	±0.08
Bi^{204}	68-min Pb^{204m}	0.0366	0.0053					
		±0.0024	±0.0004					
Bi^{205}	15-day Bi^{205}	0.0275	0.0053	0.0200	0.0160	0.0180	0.774	3.42
		±0.0003	±0.0002	±0.0005	±0.0006	±0.0004	±0.004	±0.06
Bi^{206}	6.0-day Bi^{206}	0.0220	0.0054	0.0163	0.0142	0.0153	0.745	2.92
		±0.0004	±0.0002	±0.0004	±0.0005	±0.0003	±0.004	±0.05

b. Errors quoted are random errors. For systematic errors, see text.

a. $F_P W$ is taken as the average of $F_U W$ and $F_D W$. The influence of the 10° angle between the target plane and the beam is responsible for the differences between these latter quantities.

TABLE III.

Thin-target experiments showing effect of use of gold instead of aluminum for the catcher foils. Activity measured is a mixture of mass chains 201, 202, 203, and 204 isolated in identical manner in each experiment.

Catcher foil		Experimental F_F/F_B	Calculated F_F/F_B from Monte Carlo[a]			
Backward	Forward		Uncorrected	Corrected for: Scattering	Evap.	Scat. & evap.
Al	Al	4.5 ±0.2	7.2	7.2	4.7	4.7
Al	Au	2.9 ±0.2	7.2	2.8	4.7	2.6[b]
Au	Au	3.1 ±0.2	7.2	3.3	4.7	3.1[b]
Au	Al	4.6 ±0.2	7.2	10.1	4.7	5.0[b]

a. The calculated F_F/F_B value in each case is obtained by averaging the f_F/f_B values for all events which ultimately lead to bismuth nuclei of mass numbers 199-207 inclusive, making estimates of the number of particles evaporated after the knock-on cascade.

b. Because of deficiencies of the evaporation and scattering models used, the total correction had to be estimated by combining the evaporation and scattering corrections as independent distributions, which is not a valid procedure unless one effect is very small relative to the other.

IV. THE MONTE CARLO CALCULATION

The quantities sought from the calculation for comparison with experiment are F_FW, F_BW, and F_PW of each nuclide for thick-target experiments, and F_F and F_F/F_B for thin-target experiments. First the quantities f_FW, f_BW, f_PW, and f_F for <u>each</u> recoil are obtained from the calculation. The value of F_FW, etc. for any nuclide (Z,A) will then be the average f_FW, etc. of all recoils which are destined to become final nuclei of that Z and A. ("Final nucleus" is used to signify the nucleus remaining after the evaporation process.)

The method for calculating f_FW, etc. of a given recoil, and for determining the Z and A of the final nucleus, is as follows.

The original outputs[2] of the Monte Carlo calculation are: the identity (Z,A) and excitation energy (E^*) of the <u>residual</u> nucleus (i.e. the nucleus remaining after the knock-on cascade), the kinetic energy of each emitted cascade particle (proton, neutron, and pion) as measured inside the nucleus, and two of the three direction cosines for each cascade particle. Starting with the cascade-particle energies and direction cosines, and accounting for the nuclear potential energy, Porile[9] has computed the component of momentum along the beam for each residual nucleus. He could not compute the transverse momentum component exactly, because

the Monte Carlo calculation had not kept track of the sign of the third direction cosine for each particle. Therefore he made a computation of the transverse momentum component by choosing the sign of the third direction cosine randomly, which amounts to assuming that there is no angular correlation, about the axis defined by the proton beam, between the particles in the cascade.

From the two components, the magnitude of the total momentum P_o and its direction θ_o relative to the beam can be computed for each residual nucleus. The excitation energy E^* of each residual nucleus is also known from the Monte Carlo data, from which one can estimate the number of particles evaporated and hence the Z and A of each final nucleus.

For our calculations, the estimate of the number of particles evaporated was made without considering the evaporation of particles other than neutrons. Jackson's calculations[17,18] on heavy elements indicate that proton evaporation should be small for final nuclei differing less than 10 mass numbers from the target, i.e. for excitations less than about 100 Mev.

There are, however, other evaporation calculations which indicate that, depending upon the values chosen for various input parameters, proton evaporation might be quite common. For example, using a value of 10 for the level

density parameter a, one finds that the evaporation calculation of Dostrovsky et al[19] would lead to the prediction that at 100 Mev of initial excitation one residual nucleus out of three will evaporate a proton, and a small fraction will evaporate other charged particles. This calculation was performed with a radius parameter r_o of 1.3×10^{-13} cm. Even more extensive proton (and alpha-particle) evaporation is predicted by a more recent evaporation calculation[20], which indicates that charged-particle evaporation will occur most of the time from bismuth nuclei at such initial excitations and that charged-particle evaporation is significant (i.e. one nucleus out of five) even at 40-50 Mev of initial excitation. This latter calculation was performed with a more recent program[21] which allows corrections for pairing and shell effects. Possibly this calculation[20], choosing 1.7×10^{-13} cm for the radius parameter and using Cameron's[22] pairing corrections, overestimates the extent of charged-particle evaporation, since the observed yields[4] of the lighter bismuth nuclei do not seem to be relatively low as predicted by the calculation. It does demonstrate that evaporation calculations do not provide a sound basis for ignoring proton evaporation.

The number of neutrons evaporated is calculated in the present work on the assumption that each neutron evaporation removes 11.4 Mev of excitation energy, the average amount obtained from Jackson's[18] evaporation calculations. The

number of neutrons evaporated is thus specified by the excitation of the residual nucleus. (The general features of the results of the calculations are not very sensitive to the assumption taken, as indicated by calculations made with a choice of 10 Mev per nucleon.) For residual nuclei of less than 11.4 Mev excitation, one neutron is assumed to evaporate if the excitation is greater than the neutron binding energy[22]. For excitations between 11.4 and 22.8 Mev, one neutron evaporates; for excitations between 22.8 and 34.2 Mev, two neutrons; and so on. The number of neutrons specified in this way is frequently not the maximum number that could evaporate, nor the minimum number (see refs. 17, 23, 24). In particular, one calculation[20] suggests a rather wide spread of residual nuclei for a given final nucleus. However, consideration of the various actual competing processes at a given excitation, rather than what amounts to an average process, should have little effect on the results.

If the effect of momentum imparted by evaporation is ignored, the velocity of the final nucleus can be taken to be that of the residual nucleus. If scattering is also ignored, then the value of thin-target F_F for a specific nuclide may be ascertained just from the θ_o values for the recoils leading to that nuclide.

The thick-target fW value (mg/cm^2 Bi) for the final nucleus is given by the following expressions <u>if scattering and evaporation recoil are ignored</u>:

$$f_F W = R_o \cos \theta_o \quad (\text{for } \theta_o < \tfrac{\pi}{2};\ \text{zero for } \theta_o > \tfrac{\pi}{2}) \qquad (1),$$

$$f_B W = -R_o \cos \theta_o \quad (\text{for } \theta_o > \tfrac{\pi}{2};\ \text{zero for } \theta_o < \tfrac{\pi}{2}) \qquad (2),$$

$$f_P W = (R_o \sin \theta_o)/\pi \qquad (3).$$

Here θ_o is the angle between the beam and the direction of motion of the residual nucleus as given by the Monte Carlo calculation (which is also, in this case, θ_o for the final nucleus), and the range R_o of the final nucleus (mg/cm^2 Bi) is obtained from the kinetic energy E_o by use of a range-energy relation:

$$R = 0.15\ E \qquad (4).$$

The value of E_o is given by:

$$E_o = \frac{A}{A_o} \times \frac{P_o^2}{2 \times 931.1 \times A_o} \qquad (5),$$

with A_o the mass number of the residual nucleus, A the mass number of the final nucleus, and P_o the momentum of the residual nucleus in Mev/c as given by the Monte Carlo calculation. Due to evaporation recoil, the actual θ, R, E, and P of the final nucleus may be quite different from the θ_o, R_o, E_o, and P_o obtained from the Monte Carlo calculation alone.

The effects of evaporation recoil and scattering will now be discussed.

1. Evaporation correction. Evaporation was assumed to be isotropic in the frame of the moving nucleus. Each evaporated neutron was assigned a momentum P_e of 80 Mev/c, corresponding to a kinetic energy of 3.4 Mev as dictated by the evaporation assumptions made earlier. Expressions were then derived for calculating f' and fW values for each final nucleus.

The expression for thin-target f_F for a recoil with θ_o less than $\pi/2$ (or for $1 - f_F$ if θ is greater than $\pi/2$) is:

$$f_F = 1 \qquad \text{if } n P_e < P_o \cos \theta_o \qquad (6),$$

$$f_F = 1 - 1/2 \int_{P_o \cos \theta_o}^{nP_e} \left(1 - \frac{P_o}{P_1} \cos \theta_o\right) S_n (P_1)\, d P_1 \qquad \text{if } n P_e > P_o \cos \theta_o \qquad (7).$$

Here n is the number of neutrons evaporated, P_1 is the magnitude of the resultant of the P_e vectors, and $S_n(P_1)dP_1$ is the fraction of the P_1 vectors with magnitudes between P_1 and $P_1 + dP_1$; $S_n(P_1)dP_1$ is given exactly and in Gaussian approximation by Hsiung et al[25]. (For $n = 5$ the Gaussian approximation is in good agreement with the exact expression and was used for all cases of $n > 5$.) Similarly, for thick targets, $f_F W$ and $f_B W$ are given by the sum of the following approximate expressions for $\theta_o < \pi/2$ and P_1 in the three ranges

specified. Here, $P_1(\max)$ is equal to P_o or nP_e, whichever is smaller.

$$f_F W\ (1) = \int_o^{P_1(\max)} R_o \cos\theta_o \left\{1 + \frac{2}{3}\left(\frac{P_1}{P_o}\right)^2\right\} S_n(P_1)dP_1$$

$$\text{for } P_1 < P_o \cos\theta_o \qquad (8),$$

$$f_B W\ (1) = 0$$

$$f_{\binom{F}{B}} W\ (2) = \int_{P_o\cos\theta_o}^{P_1(\max)} \left(\frac{R_o\cos\theta_o}{2}\right)\left(\frac{P_o}{P_1}\right)\left\{\frac{\cos\theta_o}{2} \pm \left(\frac{P_1}{P_o}\right) + \frac{\left(\frac{P_1}{P_o}\right)^2}{2\cos\theta_o} - \frac{\cos^3\theta_o}{12} + \frac{3}{4}\left(\frac{P_1}{P_o}\right)^2 \cos\theta_o \pm \frac{2}{3}\left(\frac{P_1}{P_o}\right)^3\right\} S_n(P_1)dP_1$$

$$\text{for } P_o\cos\theta_o < P_1 < P_o \qquad (9),$$

$$f_{\binom{F}{B}} W\ (3) = \int_{P_o}^{nP_e} \frac{Ro}{4}\left(\frac{P_1}{P_o}\right)^2 \left\{1 \pm \frac{8}{3}\left(\frac{P_o}{P_1}\right)\cos\theta_o + \frac{3}{8}\left(\frac{1}{\cos^2\theta_o} + 5\right)\left(\frac{P_o}{P_1}\right)^2 \cos^2\theta_o\right\} \times S_n(P_1)dP_1$$

$$\text{for } P_1 > P_o \qquad (10).$$

The F and FW values for each nuclide were then obtained by averaging over all the appropriate final nuclei as before. In these derivations, the small mass change of the nucleus during evaporation was neglected.

If proton evaporation is extensive, then it will affect the calculation. A proton will normally evaporate with a higher

kinetic energy than a neutron, because of the potential barrier. One consequence of this is that the evaporation process will tend to give the nucleus a much larger momentum than would be expected without proton evaporation. Another consequence of ignoring proton evaporation is that a proton generally will remove more excitation than would a neutron, thus causing the total number of particles evaporated to be smaller than would otherwise be the case. Thus proton evaporation results in a final nucleus shifted, not only one unit down in Z, but a few units upwards in A and, on the average, with a higher evaporation-recoil momentum. Thus, regardless of whether or not there are any differences in recoil behavior between isobaric Z = 83 and Z = 84 residual nuclei, proton evaporation from Z = 84 residual nuclei may very well cause the recoil properties of the Z = 83 final nuclei to be somewhat different from what they would be if proton evaporation did not occur. One mitigating factor in this problem is that the total number of Z = 84 residual nuclei from the Monte Carlo cascade calculation is smaller than the total number of Z = 83 residual nuclei so that the bulk of the Z = 83 final nuclei will come from Z = 83 residual nuclei, for any amount of proton evaporation which might be reasonably expected, even for the highest excitations in this work, ~130 Mev.

The foregoing statements also apply for the evaporation of deuterons and tritons, which are expected[19] to evaporate

less frequently. (Emission of such particles in the cascade was also ignored[2].)

Similar effects will result from the evaporation of high-energy neutrons. A recent calculation[20] indicates that, at high excitations, the probability of such neutrons may not warrant ignoring them.

2. Scattering correction.---The recoil nuclei are brought to rest by collisions with atoms of the material through which they pass. This gives rise to straggling along the initial path, the extent of which is commonly given in terms of a straggling parameter ρ, viz:

$$\rho = \sigma/R \qquad (11)$$

where R is the mean range of the particle. The probability that the particle will come to rest at some point $\underline{R}$ is commonly expressed by a Gaussian of standard deviation σ about R, i.e.:

$$W(\underline{R})\, d\underline{R} = \frac{1}{\rho R\sqrt{2\pi}} \exp\left\{-\frac{1}{2}\left(\frac{\underline{R} - R}{\rho R}\right)^2\right\} d\underline{R} \qquad (12).$$

The distribution is in fact not Gaussian[26,27] at low energies, but consists of an asymmetric peak at a value smaller than R, followed by a pronounced exponential tail. The more nearly equal the masses of the colliding particles, the more the distribution deviates from a Gaussian.

The values of ρ reported[28,29] and the theoretical predictions of ρ available[30,31] are for the distribution along the direction of initial motion of the particle. No measurements have been made upon the distribution perpendicular to the direction of the initial motion. For the recoils involved in the present study, the average $\sin \theta_o$ from the Monte Carlo calculation is 0.82, so that the lateral component of scattering is important. The following assumptions will be used in the calculations:

(1) If the stopping material is bismuth or gold, the distribution of stopped bismuth recoils along any axis is a Gaussian distribution with $\rho = 0.41$, independent of recoil energy.

(2) If the stopping material is aluminum, scattering is ignored in the thin-target case.

It can be shown that when $M_1 = M_2$, isotropic scattering will not lead to a spherically symmetric distribution as assumed in (1). In order that (2) be valid, it is only necessary that none of the distribution lie in the backward foil. This condition is very nearly met in the thin-target case, because the average energy transfer and deflection per collision are both small for bismuth moving through aluminum ($M_1 >> M_2$).

The case where aluminum catchers are used with a thick bismuth target or where, in the thin-target case, one catcher

is aluminum and the other is gold, presents a special problem in that stopping is taking place in media of $M_1 \sim M_2$ as well as $M_1 >> M_2$. Further assumptions had to be made for the case of thick target and aluminum catchers. For example, straggling in aluminum, both along and across the line of flight, was assumed to be negligible; the other assumptions will be omitted from the discussion for the sake of brevity.

For the thin-target case where one catcher is aluminum and the other is gold, the following is assumed:

(3) If a recoil from the thin target initially enters the gold catcher, f_F and f_B are the same whether the other catcher is gold or aluminum. (If it enters the aluminum catcher, assumption (2) applies, i.e. f_F and f_B are the same as if both catchers were aluminum.)

This assumption implies that assumption (1) still holds even if the tail of the Gaussian scatter distribution lies in aluminum rather than in gold. Thus, the foils should act independently in their effect on F_F and F_B. If this is true, then it should be possible to determine any one of the F_F/F_B ratios in Table III from the other three. Within experimental error this is the case.

The justification for (3) is as follows: If the recoil enters the gold catcher, then $M_1 \sim M_2$, so that the recoil undergoes a deflection of $\pi/4$ and gives up half its energy in

each collision, on the average. Since at these energies total path length is roughly linear with energy[26,27,30-32], the recoil travels one-half its total path length before making the first collision, on the average, half the remainder before the second, etc. The final stopping place for the recoil is thus determined by the first few collisions. For a recoil moving initially into the gold catcher foil and then coming to rest in the other foil, the first few collisions will have taken place in the gold foil and the influence of the other foil will be relatively unimportant. Hence assumption (3).

Finally, for calculating $f_P W$ it proved difficult to use the Gaussian distribution of (1), so the following assumption was made:

(4) For $f_P W$, the recoils end up on the surface of a sphere of radius 0.41 R centered at R.

This assumption applies for gold catchers. No experiments or calculations for $f_P W$ with aluminum catchers were made. If this assumption is used for calculating $f_F W$ or $f_B W$, it leads to scattering corrections only about 30% as great as those calculated with the Gaussian distribution, on the average, and it shows also that, on the average, the effect of scattering on the value of $f_P W$, in terms of a [illegible] about twice the fractional percent of $f_P W$, is about twice as great as the effect on $f_F W$, as a percent of $f_F W$. The scattering correction calculated for $f_P W$ is, therefore,

smaller than it should be.

Using the foregoing assumptions, expressions were obtained for calculating f and fW for a specific recoil from the Monte Carlo calculation. Here θ is the angle between the beam and the initial direction of motion of the recoil. Because of scattering, R is no longer unique but is the mean of a distribution. Because of evaporation recoil, R and θ may differ considerably from the range R_o and angle θ_o obtained from the Monte Carlo calculation alone.

(a) For thin target, aluminum forward catcher, f_F is unity.

(b) For thin target, gold forward catcher,

$$f_F = \frac{1}{\rho R\sqrt{2\pi}} \int_{-R\cos\theta}^{\infty} \exp\left(-\frac{x^2}{2\rho^2 R^2}\right) dx \qquad (13),$$

(c) For thick target, gold catchers,

$$f_F W = R\cos\theta + \delta \qquad (14),$$

$$f_B W = \delta \qquad (15),$$

where

$$\delta = \frac{\rho R}{\sqrt{2\pi}} \exp\left[-\frac{1}{2}\left(\frac{\cos\theta}{\rho}\right)^2\right] - \frac{R\cos\theta}{\rho R\sqrt{2\pi}} \int_{-\infty}^{-R\cos\theta} \exp\left(-\frac{x^2}{2\rho^2 R^2}\right) dx \qquad (16).$$

The above expressions apply for a recoil with $\theta < \pi/2$. For a recoil with $\theta > \pi/2$, they apply with F and B interchanged.

Finally, for any value of θ,

$$f_P W = \begin{cases} \frac{3}{4\pi}\left(R^2\sin^2\theta - r^2\right)^{1/2} + \frac{1}{4\pi r}\left(R^2\sin^2\theta + 2r^2\right)\sin^{-1}\left(\frac{r}{R\sin\theta}\right) & \text{if } \sin\theta \geq \frac{r}{R} \quad (17), \\ \frac{R^2\sin^2\theta}{8r} + \frac{r}{4} & \text{if } \sin\theta < \frac{r}{R} \quad (18), \end{cases}$$

where $r = 0.41R$ is the radius of the spherical scattering distribution in accordance with assumption (4).

Equations (14) and (15) show that δ, the scattering correction for a given recoil, is the same for both $f_B W$ and $f_F W$. It can be shown that, regardless of the shape of the distribution, for a thick target where the atoms of the target and the catcher material have the same mass, the scattering correction δ is always the same for both $f_F W$ and $f_B W$. It can also be proved that δ is greater than zero if part of the distribution lies behind the point where the recoil originates, measuring along a direction perpendicular to the interface, and that otherwise δ is zero.

The validity of expressions (13) through (18) requires that the mean of the distribution along the beam axis be $R\cos\theta$, and similarly $R\sin\theta$ for the perpendicular projection. This requirement is met as long as the distribution is symmetric about some axis.

Associated with the problem of straggling is the determination of R itself. After a review of the experimental [13,27,29,33] and theoretical [31,32] work bearing on the subject, the assumption was adopted that R is proportional to kinetic energy for these recoil energies, with a proportionality factor of 0.15 as given in Equation (4).

Inclusion of evaporation recoil and scattering in the calculations produces a large effect, as may be seen from the last three columns of Table III for the thin-target case and in Figs. 3 and 4 for the thick-target case. Combining the scattering and evaporation-recoil effects is difficult, first because the distribution of recoils from scattering is not truly Gaussian, as used in the calculation. Secondly, the distribution of the projection of recoils resulting from the evaporation is quite skewed except for large values of R. Third, the effects are not independent, in that the σ of the scattering distribution is not fixed for a given recoil but varies with the resultant of the Monte Carlo momentum and the various possible momenta from evaporation recoil.

Accordingly, there is no really valid way to combine the two corrections. For the thin-target case (Table III), the effects are combined by assuming that the square of the combined effect for F_F is equal to the sum of the squares of the two independently. The error of doing this is not too serious, since one effect or the other is always dominant in

the thin-target case — scattering when the forward catcher is gold, evaporation when it is aluminum. Scattering predominates for F_BW in the thick-target case (Fig. 4); however for F_FW (Fig. 3) scattering and evaporation effects are comparable, so this procedure cannot be used. Therefore the calculation is corrected only for scattering in the thick-target case.

V. COMPARISON OF CALCULATION AND EXPERIMENT

The thin-target data reported in Table III for the $Bi^{201-204}$ mixture demonstrate that scattering is important. Included in the table for comparison are values from the Monte Carlo calculation for a $Bi^{199-207}$ mixture, which should be a good representation for the $Bi^{201-204}$ mixture. (The latter is mostly 203 and 204.) In the column headed "uncorrected" is the F_F/F_B value calculated for this mixture with no correction for evaporation recoil or scattering. The next column shows this value with scattering taken into account. The value with consideration of evaporation recoil alone is shown in the following column. In the last column are estimates of the F_F/F_B values with evaporation recoil and scattering both considered. The difficulties of combining the effects have already been discussed. The F_F/F_B value which would be obtained with a more proper combining procedure would probably differ from the listed values by less than 0.3. The rather good agreement between the experimental results

and the figures of this last column suggests that the effects of evaporation recoil and scattering are adequately treated by the methods used in the calculation for dealing with them.

Calculated and experimental values of F_F for aluminum catchers (Fig. 5 and Table IV) are in good agreement, both in the magnitudes of F_F and in their trend with mass number.

Calculation and experiment are in good accord for F_FW and F_BW with gold catchers (Fig. 6 and Table IV), both in magnitude and in trend with mass number. It appears that F_BW is due almost entirely to scattering, which explains why its value is about 0.0055, irrespective of mass number.

However, the scattering model is not successful in predicting the experimental fact that there is no difference between the values of F_FW and F_BW obtained with gold catchers and those obtained with aluminum catchers. Any reasonable evaluation of scattering leads to the prediction that there should be an observable difference, particularly for F_FW (say, 10%). The deficiency of the model might be the result of the neglect of straggling in aluminum along the initial direction of motion, which may have a large effect in the thick-target case even if it does not have a significant effect in the thin-target case where all the recoils originate at the interface.

Experimental and calculated F_pW data are compared in Fig. 7 and Table IV. Although it is perhaps not apparent in Fig. 7, the Monte Carlo calculations, in general, predict[9] only a slight increase in F_pW with decreasing mass number. Apart from the matter of trend, there appears to be only fair agreement between the calculated and experimental data. Correction for evaporation recoil and a more realistic scattering correction would increase the disagreement.

A better comparison of calculation and experiment is afforded by Fig. 8, which shows calculated and experimental F_pW/F_FW ratios. (One advantage of plotting the ratio, rather than the FW values alone, is that the ratio is less sensitive to the assumptions, approximations, and extraordinarily large or small recoil momenta in the calculations, as well as to the systematic errors in the experiments.) It may be seen in Fig. 8 that the experimental ratios are slightly lower than the calculated ones — the difference would be larger if a proper estimate of scattering had been made in the F_pW calculations — and the difference seems to increase with mass number. These observations imply that the experimental F_pW values are lower than the calculated ones, particularly at the higher mass numbers (Fig. 7). This presumably means that the calculation[9] overestimates the average transverse momentum imparted in the knock-on cascade, particularly at the higher mass numbers.

TABLE IV.

Results of the calculation for bismuth recoils.

Mass No.	No. of events	$F_B W$		$F_B W$		$F_B W$		F_B	
		Calc.[a]	Expt.	Calc.[a]	Expt.	Calc.[b]	Expt.	Calc.[c]	Expt.
198	15	0.11609		0.00194	---	0.03003	--		--
		±0.02329[d]		±0.00046		±0.00682			
199	11	0.02675	0.08[e]	0.00184	0.007[e]	0.01293	--	0.838	--
		±0.00655		±0.00104		±0.00246		±0.054	
200	12	0.05291	0.07[e]	0.00152	0.007[e]	0.02242	--	0.963	--
		±0.00809	(Bi+Pb)	±0.00043	(Bi+Pb)	±0.00437		±0.015	
201	10	0.06686	0.05[e]	0.00670	~0.007[e]	0.03089	---	0.831	--
		±0.01950	(Bi+Pb)	±0.00259	(Bi+Pb)	±0.00559		±0.099	
202	12	0.03733	--	0.00440	---	0.02130	--	0.746	--
		±0.00847		±0.00147		±0.00372		±0.089	
203	17	0.05325	0.0434[f]	0.00990	0.0057[f]	0.04836	0.0239[f]	0.901	0.8275[g]
		±0.01168	±0.0004	±0.00316	±0.0002	±0.01234	±0.0006	±0.035	±0.0027
204	11	0.03893	0.0366[f]	0.00417	0.0053[f]	0.02411	---	0.935	--
		±0.00619	±0.0024	±0.00144	±0.0004	±0.00388		±0.031	
205	9	0.02681	0.0275[f]	0.00799	0.0053[f]	0.02510	0.0180[f]	0.804	0.774[g]
		±0.00818	±0.0003	±0.00343	±0.0002	±0.01030	±0.0004	±0.107	±0.004
206	15	0.01432	0.0220[f]	0.00533	0.0054[f]	0.01300	0.0153[f]	0.675	0.745[g]
		±0.00348	±0.0004	±0.00178	±0.0002	±0.00237	±0.0003	±0.084	±0.004
207	18	0.02508	---	0.00936	--	0.02593	--	0.764	--
		±0.00695		±0.00294		±0.00815		±0.092	
208	7	0.00500	---	0.00663	---	0.00648	--	0.456	--
		±0.00204		±0.00260		±0.00165		±0.168	

d. Calculated errors reflect only the spread of the data, and do not include errors associated with the approximations and assumptions used in the calculation.

a. Calculation for gold catchers; includes Gaussian scattering model, no evaporation recoil.

b. Calculation for gold catchers; includes "ball-model" scattering, no evaporation recoil.

c. Calculation for aluminum catchers; ignores scattering and includes evaporation recoil.

e. Experimental data of Sugarman et al (ref. 14) using aluminum catchers.

f. Results of this work using gold catchers.

g. Results of this work using aluminum catchers.

The difficulty may lie in the assumption[9] that there is no directional correlation, about the beam axis, between emitted cascade particles. If instead the particles are correlated, as is obviously the case for a cascade in which two particles collide and leave the nucleus without further collisions, then the assumption will lead to calculated F_PW values which are too large. For more extensive cascades, which generally lead to final nuclei of lower mass number, the correlation among emitted particles should be weaker and hence the assumption should lead to less difficulty at the lower mass numbers, congruous with observation.

Measurements of transverse momentum for other species[34,35] appear to be in good agreement with the calculations[9]. The Monte Carlo calculations[2] have been repeated[12] for the $Al^{27}(p,3pn)Na^{24}$ reaction at 360 and 1840 Mev bombarding energy, anticorrelating the directions of the first two cascade particles. The results for F_PW, as well as for F_FW and F_BW, are in poor agreement with the experimentally established values at 1840 Mev (ref. 12; see also references quoted therein). Agreement at 360 Mev is better, but angular distribution measurements[12] indicate that this agreement is only accidental.

Measurements of the average forward momentum imparted to uranium nuclei by 460- and 660-Mev protons give values[35,36] somewhat lower than the calculated[9] ones. This has been interpreted[9] to mean that the Monte Carlo calculation fails

to predict sufficient probability for collisions of bombarding particle and target with transfer of very small amounts of forward momentum (and excitation). The present work does not bear upon this interpretation, since it is not clear how the recoil properties should be affected in consequence of this interpretation. Measurements of forward momentum imparted to emulsion nuclei[34,37] seem to concur with the calculations[9].

Use of the data as a more severe test of present concepts of high energy nuclear reactions must await a better treatment of the stopping process and a Monte Carlo calculation with more events and with explicit transverse momentum information.

ACKNOWLEDGMENTS

We wish to acknowledge the cooperation of the director and operating crew of the University of Chicago synchrocyclotron. For giving freely of their time and ideas on our behalf, we are grateful to Dr. Lester Winsberg, Dr. John M. Alexander, Dr. Helmut Münzel, Dr. Arthur Poskanzer, Dr. Norbert Porile, and Professor Anthony Turkevich.

APPENDIX. CHEMICAL PROCEDURES.

The foils were dissolved in appropriate acids (conc. HNO_3 for Bi, conc. HCl for Al, aqua regia for Au) and known weights of bismuth carrier added. The solutions were then diluted and portions were taken for analysis. Lead holdback carrier was added and bismuth was isolated from these solutions by the following steps: BiOCl precipitation, CuS scavenge from 6N HCl (removes Po, which would come through otherwise, and Mo), Bi_2S_3 precipitation from 2.4N HCl, two Bi_2S_3 precipitations with NH_4S_x (removes Sn), a second CuS scavenge from 6N HCl, a second Bi_2S_3 precipitation from 2.4N HCl, two $PbCrO_4$ scavenges from a buffered (NH_4Ac-HAc) solution, two more BiOCl precipitations, and a $BiPO_4$ precipitation from 0.5N HNO_3. This last step offers no decontamination of any importance but is quantitative and fast so that all samples may be precipitated simultaneously, gives a stoichiometric and easily-filtered precipitate suitable for weighing, and leaves Pb in solution so that subsequent Pb growth will be from an initially pure parent fraction. Decontamination from Pb is afforded by the BiOCl, Bi_2S_3 (from 2.4N HCl), and $BiPO_4$ precipitations and the $PbCrO_4$ scavenges. Yields were about 80%.

For the subsequent separation of lead daughters, the $BiPO_4$ precipitate was dissolved in HCl, Pb carrier added, and Bi was removed by a BiOCl precipitation. Then $PbO(H_2O)_x$ was precipitated with NH_3 and purified by a $BiPO_4$ scavenge, a $PbSO_4$

precipitation, and a $PbCrO_4$ precipitation from buffered solution. The Pb was weighed and counted as $PbCrO_4$. Yields were about 80%.

The bismuth activity, as BiOCl from the lead separation, was dissolved in HCl and decontaminated from daughter activities by two precipitations of BiOCl and one of $BiPO_4$, in which form it was weighed and counted.

The effectiveness of these procedures was checked by tracer experiments on the various steps and by taking gamma-ray spectra, with a multichannel analyzer, of samples separated from irradiated target and catcher foils. Activation corrections were rather constant, say 1% of F_BW for thick target and gold catchers.

* This work was supported in part by a grant from the U. S. Atomic Energy Commission.

† Present address: Scientific Laboratory, Ford Motor Company, Dearborn, Michigan.

REFERENCES

1. R. Serber, Phys. Rev. 72, 1114 (1947).
2. N. Metropolis, R. Bivins, M. Storm, A. Turkevich, J. M. Miller, and G. Friedlander, Phys. Rev. 110, 185 (1958); N. Metropolis, R. Bivins, M. Storm, J. M. Miller, G. Friedlander, and A. Turkevich, Phys. Rev. 110, 204 (1958).
3. W. E. Bennett, Phys. Rev. 94, 997 (1954).
4. E. T. Hunter and J. M. Miller, Phys. Rev. 115, 1053 (1959).
5. For a review and for further references up to Feb. 1959 see J. M. Miller and J. Hudis, Ann. Rev. Nuclear Sci. 9, 159 (1959).
6. T. U. Malysheva and I. P. Alimarin, Soviet Phys.—JETP 35, 772 (1959);
   A. K. Lavrukhina, L. P. Moskaleva, L. D. Krasavina, and I. M. Grechishcheva, J. Nucl. Energy 8, 231 (1959);
   H. P. Yule and A. Turkevich, Phys. Rev. 118, 1591 (1960);
   P. A. Benioff, Phys. Rev. 119, 316 (1960);
   P. A. Benioff, Phys. Rev. 119, 324 (1960);
   I. Ladenbauer and L. Winsberg, Phys. Rev. 119, 1368 (1960);
   D. R. Nethaway and L. Winsberg, Phys. Rev. 119, 1375 (1960);
   [illegible]
   A. K. Lavrukhina and A. A. Pozdnyakov, Reactor Sci. 13, 88 (1960);
   M. Lefort, G. Simonoff, and X. Tarrago, J. Phys. Radium 21, 388 (1960);
   N. Poffé, G. Albouy, R. Bernas, M. Gusakow, M. Riou, and

J. Teillac, J. Phys. Radium 21, 343 (1960);

M. Lefort, Comptes Rend. 253, 2221 (1961);

C. Riehl, J. Phys. Radium 22, 770 (1961);

M. Gusakow, G. Albouy, N. Poffé, and C. Riehl, J. Phys. Radium 22, 636 (1961);

N. Poffé, G. Albouy, M. Gusakow, and J. L. Sarrouy, J. Phys. Radium 22, 639 (1961);

P. P. Strohal and A. A. Caretto, Jr., Phys. Rev. 121, 1815 (1961);

W. R. Ware and E. O. Wiig, Phys. Rev. 122, 1837 (1961);

B. D. Pate and A. M. Poskanzer, Phys. Rev. 123, 647 (1961);

T. M. Kavanagh and R.E.Bell, Can.J.Phys. 39, 1172 (1961);

N. T. Porile, Phys. Rev. 125, 1379 (1962);

S. Kaufman, Phys. Rev. 126, 1189 (1962);

J. Robb Grover, Phys. Rev. 126, 1540 (1962);

D. L. Morrison and A. A. Caretto, Jr., Phys. Rev. 127, 1731 (1962);

S. Singh and J. M. Alexander, Phys.Rev.128, 711 (1962).

7. B. N. Belyaev, A. V. Kalyamin, and A. N. Murin, Soviet Phys.— Doklady 6, 784 (1962).

8. N. T. Porile and N. Sugarman, Phys. Rev. 107, 1410 (1957).

9. N. T. Porile, Phys. Rev. 120, 572 (1960).

10. L. V. Volkova and F. P. Denisov, Soviet Phys.— JETP 35, 538 (1958).

11. E. R. Merz and A. A. Caretto, Jr., Phys. Rev. 126, 1173 (1962).

12. A. M. Poskanzer, J. B. Cumming, and R. Wolfgang, Phys. Rev. 000, 0000 (0000).

13. For a review of the recoil technique, see B. G. Harvey, Ann. Rev. Nuclear Sci. 10, 235 (1960).

14. N. Sugarman, M. Campos, and K. Wielgoz, Phys. Rev. 101, 388 (1956).

15. C. Sakoonkim, private communication (1961).

16. Nuclear Data Sheets, National Academy of Sciences-National Research Council (U. S. Govt. Printing Office, Wash., D.C., 1958 et seq).

17. J. D. Jackson, Can. J. Phys. 34, 767 (1956).

18. J. D. Jackson, Can. J. Phys. 35, 21 (1957).

19. I. Dostrovsky, P. Rabinowitz, and R. Bivins, Phys. Rev. 111, 1659 (1958).

20. These calculations were kindly performed by L. Altman, R. Korteling and J. M. Alexander (private communication, 1962).

21. I. Dostrovsky, Z. Fraenkel, and G. Friedlander, Phys. Rev. 116, 683 (1960).

22. A. G. W. Cameron, Can. J. Phys. 35, 1021 (1957); Atomic Energy of Canada Limited Report CRP-690.

23. R. Vandenbosch, J. R. Huizenga, W. F. Miller, and E. M. Keberle, Nuclear Phys. 25, 511 (1961).

24. M. Lindner and A. Turkevich, Phys. Rev. 119, 1632 (1960).

25. C.-H. Hsiung, H.-C. Hsiung, and A. A. Gordus, J. Chem. Phys. 34, 535 (1961).

26. J. A. Davies, J. D. McIntyre, R. L. Cushing, and M. Lounsbury, Can. J. Chem. 38, 1535 (1960).

27. J. A. Davies and G. A. Sims, Can. J. Chem. 39, 601 (1961).

28. R. B. Leachman and H. Atterling, Arkiv Fysik 13, 101 (1957).

29. L. Winsberg and J. M. Alexander, Phys. Rev. 121, 518 (1961).

30. N. Bohr, Kgl. Danske Videnskab. Selskab, Mat.-fys. Medd. 18, No. 8 (1948).

31. J. Lindhard and M. Scharff, Phys. Rev. 124, 128 (1961).

32. K. O. Nielsen, Electromagnetically Enriched Isotopes and Mass Spectrometry, M. L. Smith, editor (Academic Press, Inc., New York, 1956), p. 68.

33. R. A. Schmitt and R. A. Sharp, Phys. Rev. Letters 1, 445 (1958); B. G. Harvey, W. H. Wade, and P. F. Donovan, Phys. Rev. 119, 225 (1960); V. A. J. van Lint, R. A. Schmitt, and C. S. Suffredini, Phys. Rev. 121, 1457 (1961).

34. V. I. Ostroumov, Soviet Phys.—JETP 5, 12 (1957).

35. A. I. Obukhov, Soviet Phys.—JETP 8, 727 (1959).

36. N. A. Perfilov, N. S. Ivanova, O. V. Lozhkin, V. I. Ostroumov, and V. P. Shamov, Proceedings of the Conference of the Academy of Sciences U.S.S.R. on the Peaceful Uses of Atomic Energy, July 1, 1955 (Akademia Nauk S.S.S.R., Moscow, 1955), p. 55 (translated by the Consultants Bureau, New York: Atomic Energy Commission Report TR-2435, 1956); N. S. Ivanova and I. I. Pianov, Soviet Phys.—JETP 4, 367 (1957).

37. E. W. Baker, S. Katcoff, and C. P. Baker, Phys. Rev. 117, 1352 (1960).

FIGURE CAPTIONS

Fig. 1. Thick-target assemblies, showing the two orientations used for studying recoil behavior: (a) forward-backward and (b) perpendicular.
G, guard foil; B, backward catcher foil; T, target; F, forward catcher foil; A, activation foil.

Fig. 2. Thin-target assembly.
G, guard foil; B, backward catcher foil; T, target; F, forward catcher foil; A, activation foil.

Fig. 3. Monte Carlo calculations of $F_F W$, showing effects of inclusion of scattering (gold catchers) and evaporation recoil in the calculations. (Error flags are omitted.)
Δ,....., corrected for scattering only; O,-----, corrected for evaporation only; ●,———, uncorrected.

Fig. 4. Monte Carlo calculations of $F_B W$, showing effects of inclusion of scattering (gold catchers) and evaporation recoil in the calculations. (Error flags are omitted.)
Δ,....., corrected for scattering only; O,----, corrected for evaporation only; ●,———, uncorrected.

Fig. 5. Comparison of experimental and calculated thin-target F_F values (see Table IV), aluminum catchers. Evaporation recoil is included in the calculation, and scattering

is assumed to have a negligible effect.

 , Monte Carlo calculation, corrected for evaporation recoil; ⊙, experimental value.

Fig. 6. Comparison of experimental and calculated $F_F W$ and $F_B W$ (see Table IV). A Gaussian scattering distribution is assumed in the calculation, with $\rho = 0.41$ along all axes. Momentum transfer from evaporation is ignored. (Error flags show only the spread of the calculated data, and do not include errors associated with approximations and assumptions used in the calculation.)

 , calculated, with scattering correction but no evaporation recoil correction; ⊙, experiment this work (errors not shown); □, experiment, Sugarman et al (Ref. 14). Values at A=200 and 201 are for mixed Bi and Pb recoils.

Fig. 7. Comparison of experimental and calculated $F_P W$ (see Table IV). A "ball model" scattering is assumed in the calculation, with $\rho = (6)^{-\frac{1}{2}}$. Recoil from evaporation is ignored.

 , Monte Carlo calculation, corrected for scattering; ⊙, experimental value.

Fig. 8. Comparison of experimental and calculated $F_P W/F_F W$ ratios (with scattering).

 , Monte Carlo calculation; ⊙, experimental value.

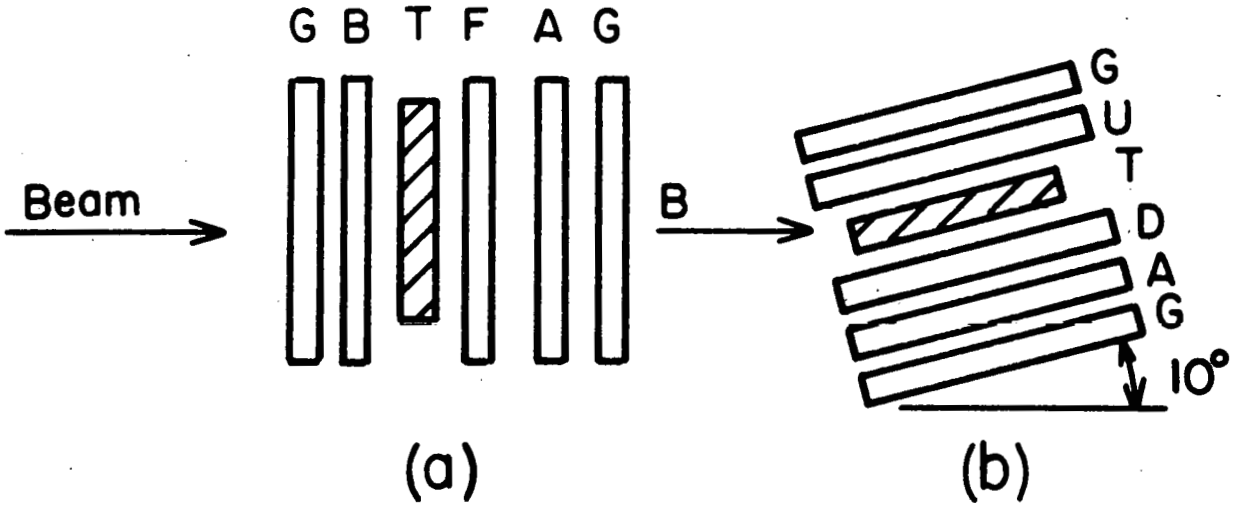

Fig.1

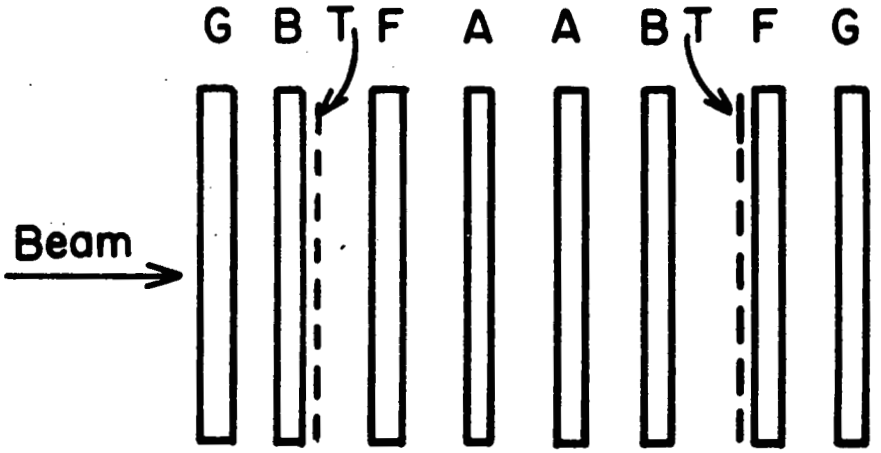

Fig.2

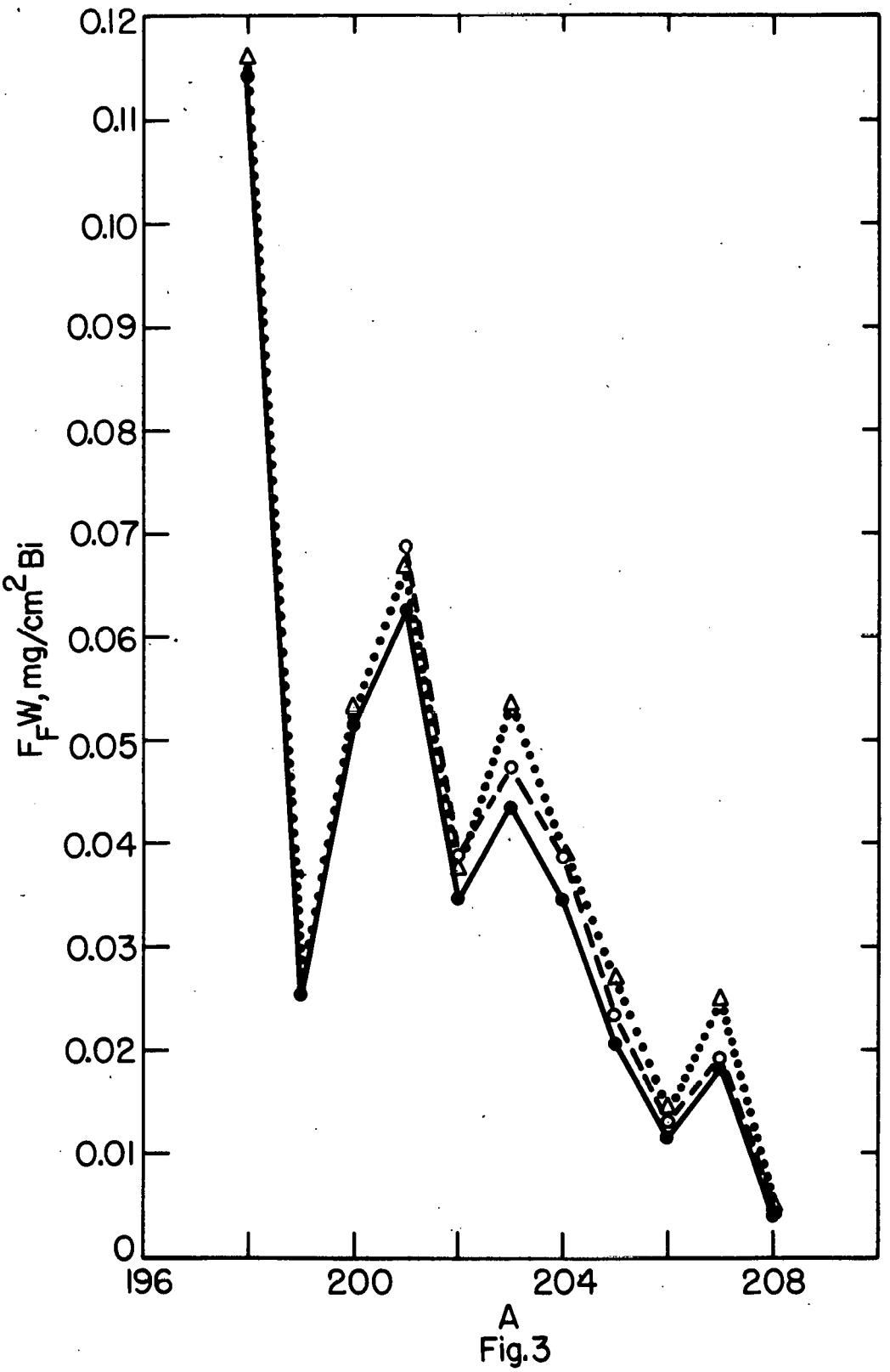
0.12
0.11
0.10
0.09
0.08
0.07
0.06
0.05
0.04
0.03
0.02
0.01
0
$F_F W$, mg/cm^2 Bi
196
200
204
208
A

Fig.3

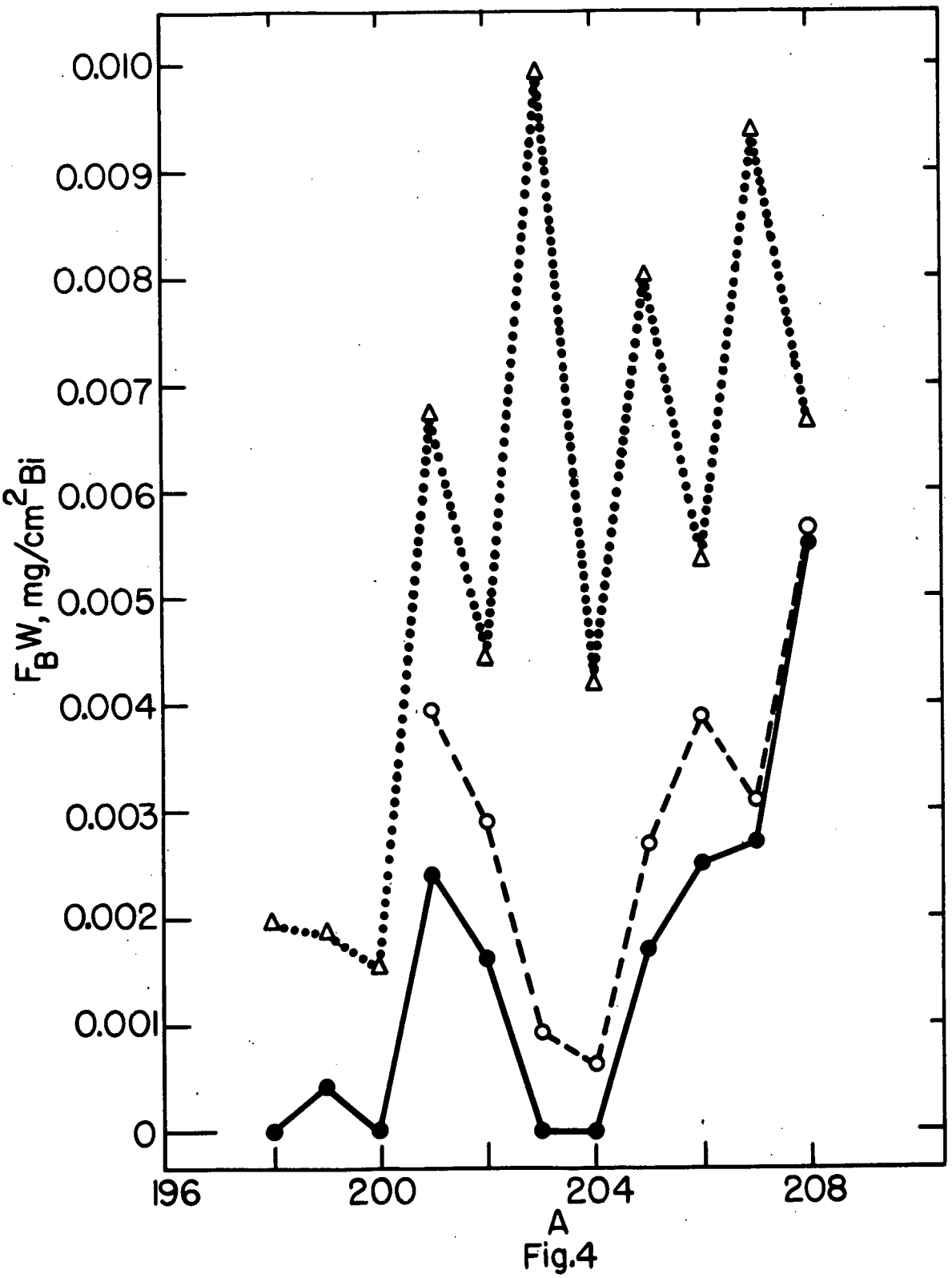
0.010
0.009
0.008
0.007
0.006
0.005
0.004
0.003
0.002
0.001
0
$F_B W$, mg/cm^{2}Bi
196
200
204
208
A

Fig.4

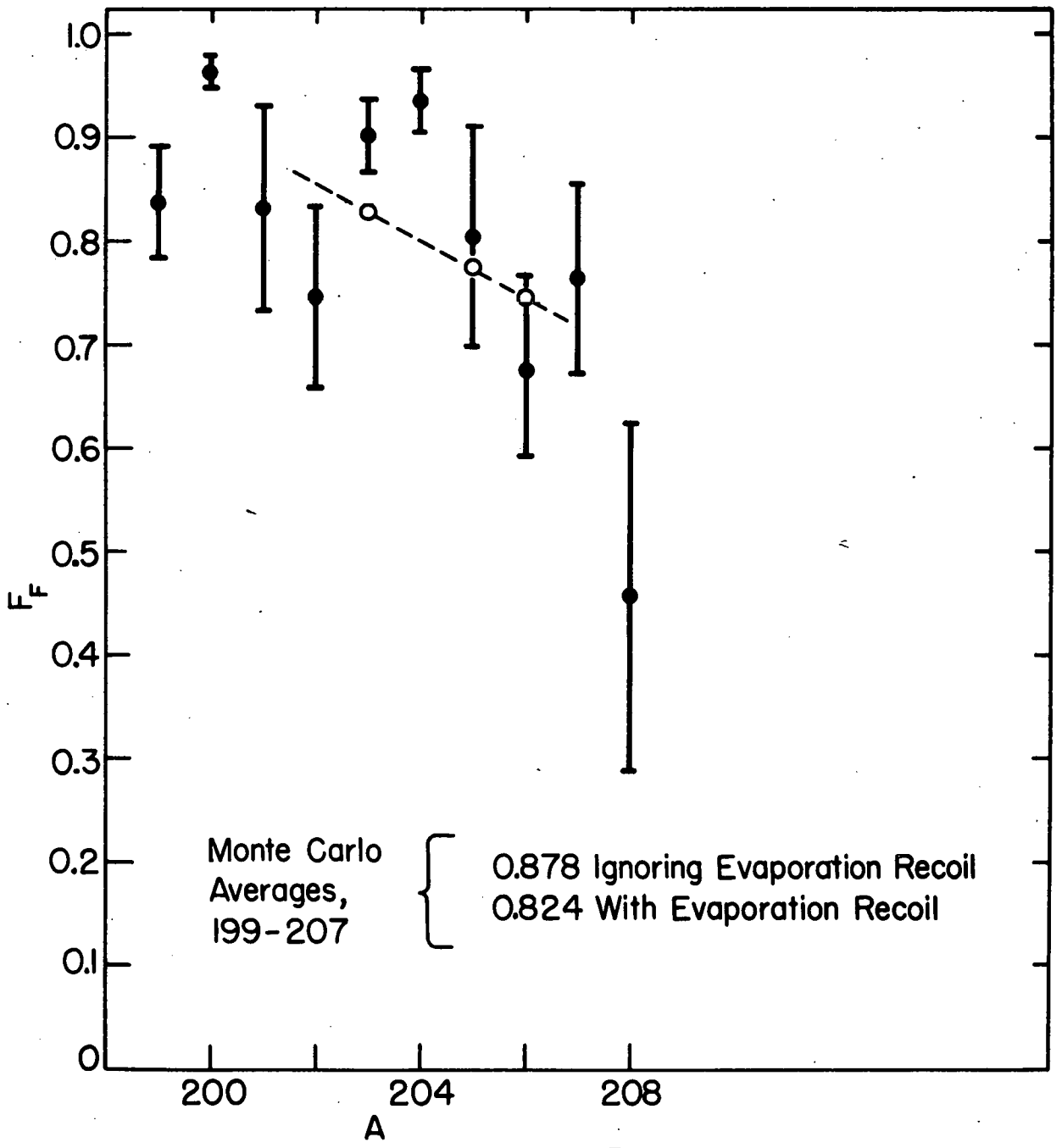
1.0
0.9
0.8
0.7
0.6
0.5
0.4
0.3
0.2
0.1
0
F_F
200
204
208
A
Monte Carlo
Averages,
199-207
0.878 Ignoring Evaporation Recoil
0.824 With Evaporation Recoil

Fig.5

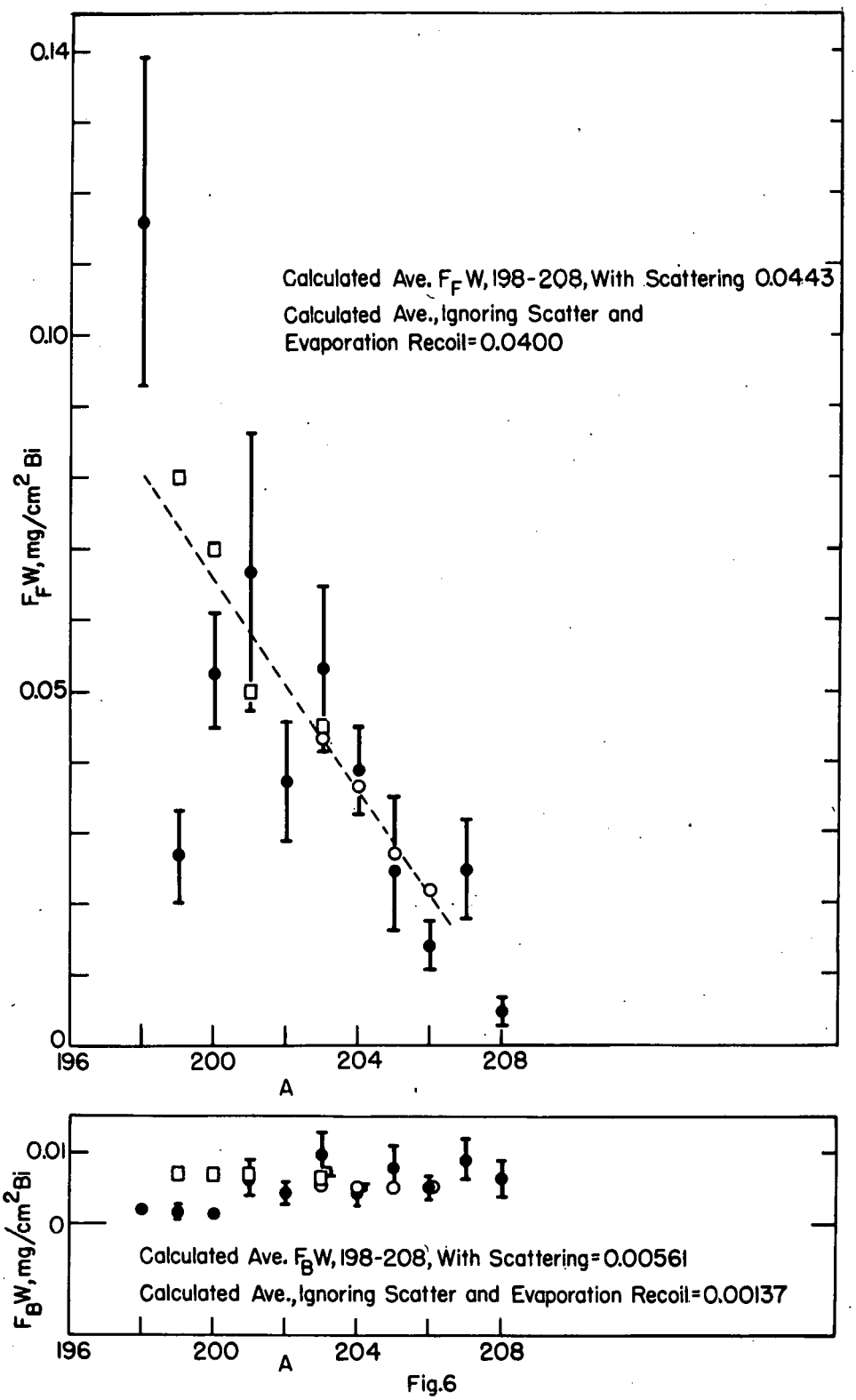
0.14
0.10
0.05
0
$F_F W$, mg/cm^2 Bi
Calculated Ave. $F_F W$, 198-208, With Scattering 0.0443
Calculated Ave., Ignoring Scatter and
Evaporation Recoil=0.0400
196
200
204
208
A
0.01
0
$F_B W$, mg/cm^2 Bi
Calculated Ave. $F_B W$, 198-208, With Scattering=0.00561
Calculated Ave., Ignoring Scatter and Evaporation Recoil=0.00137
196
200
204
208
A

Fig.6

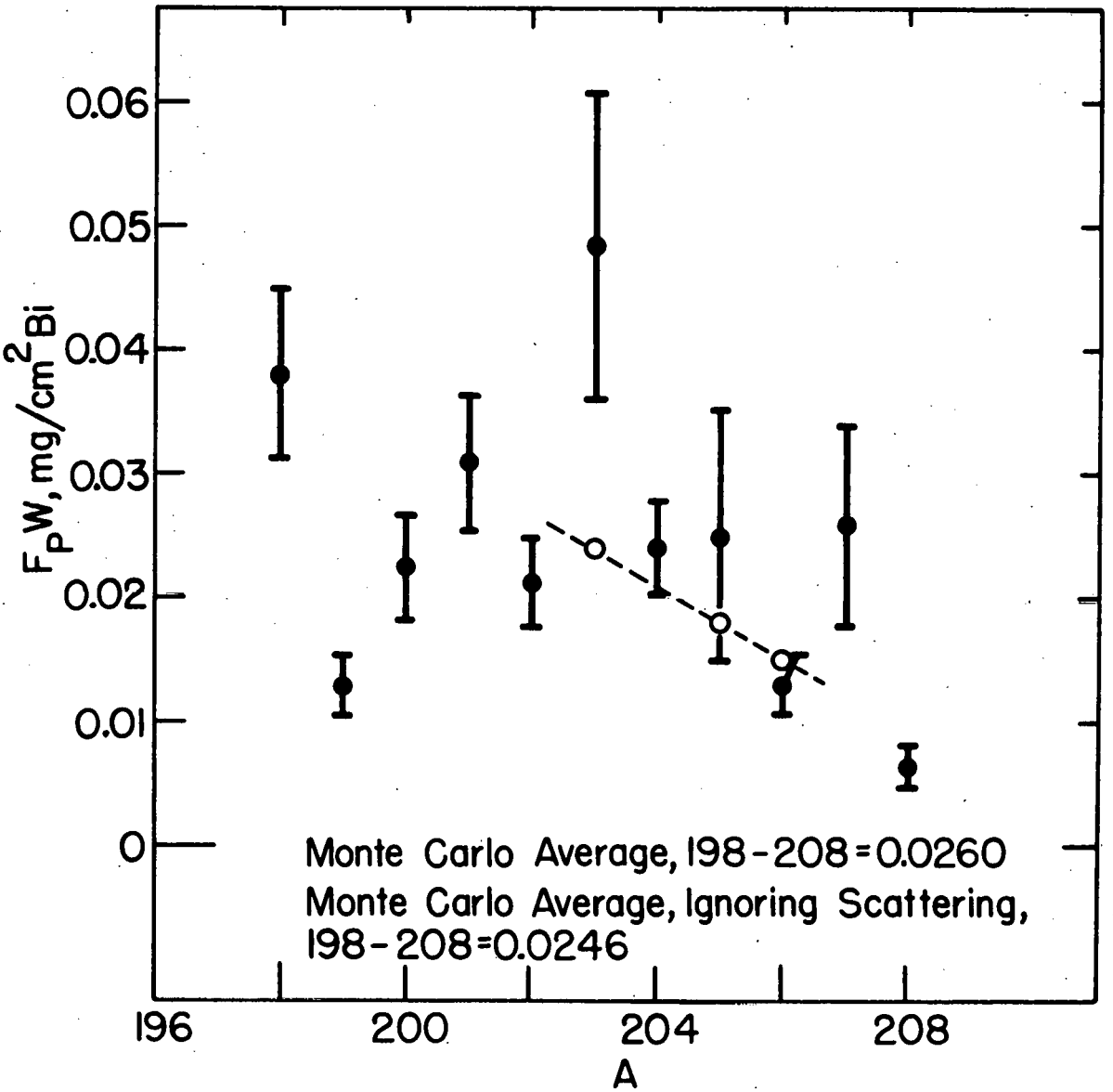
0.06
0.05
0.04
0.03
0.02
0.01
0
F_pW, mg/cm^{2}Bi
Monte Carlo Average, 198-208=0.0260
Monte Carlo Average, Ignoring Scattering,
198-208=0.0246
196
200
204
208
A

Fig.7

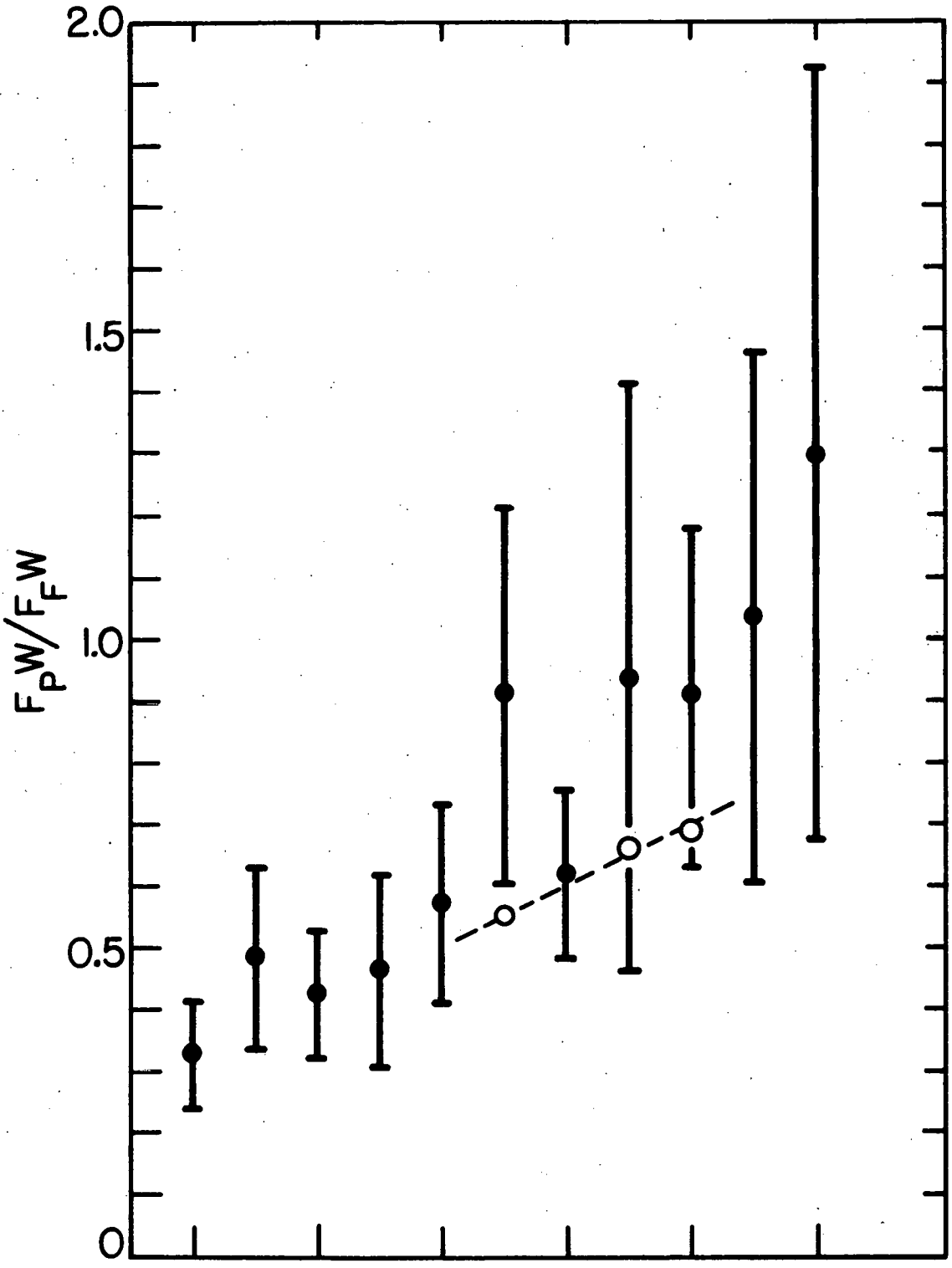

Fig.8